Measurement 93 (2016) 258–264

Contents lists available at ScienceDirect

Measurement

journal homepage: www.elsevier.com/locate/measurement

Leap motion controller three dimensional verification and polynomial correction

Yajaira-Ilse Curiel-Razo [a], Octavio Icasio-Hernández [a,b], Gabriel Sepúlveda-Cervantes [c], Juan-Bautista Hurtado-Ramos [a], José-Joel González-Barbosa [a,*]

[a] Instituto Politécnico Nacional, CICATA, Unidad Querétaro, Cerro Blanco No. 141, Col. Colinas del Cimatario, 76090 Querétaro, Mexico
[b] Centro Nacional de Metrología, CENAM, km 4.5 Carretera a Los Cués, Municipio El Marqués, 76246 Querétaro, Mexico
[c] Instituto Politécnico Nacional, CIDETEC, Av. Juan de Dios Bátiz s/n esq, Miguel Othón de Mendizábal, Col. Nueva Industrial Vallejo, Del., Gustavo A. Madero, 07700 CD México, Mexico

ARTICLE INFO

Article history:
Received 10 March 2015
Accepted 5 July 2016
Available online 7 July 2016

Keywords:
Dimensional verification
Error
Leap motion controller
Polynomial correction
Uncertainty

ABSTRACT

We propose a leap motion controller (LMC) dimensional verification based on ISO 10360-2:2009 with a coordinated measuring machine (CMM) as the reference framework. A pointer device comprising a thin aluminum cylinder was used to simulate a human finger. This was mounted on the spindle of the CMM to mark known positions over the LMC workspace. Polynomial tendency line corrections were applied to reduce the error in the LMC and CMM framework alignment. One dimension verification results were less than 0.1 mm in the *X* and *Z* axes, whereas the *Y* axis produced unsuitable results. The mean error was 9.6 mm in three-dimensional (3D) verification. Our findings demonstrate the difference between manufacturer quoted accuracy (0.01 mm) to that practically obtainable when the pointer was placed in a known position. LMC needs to add tracking models and position error compensation in applications requiring high accuracy, such as industrial processes or surgical procedure simulations.

1. Introduction

Hand movements are being exploited by gesture recognition techniques and motion gesture sensors (MGS) to create or improve human-computer interaction (HCI) and natural user interfaces (NUI) [1]. The desire for HCIs that are increasingly natural for the user has stimulated research on hand gesture recognition. Improvements in HCI encourage the design and development of efficient and accurate recognition systems, capable of identifying any minimum gesture as input to the system.

Microsoft Kinect is a consumer-grade MGS that enables user interaction without requiring a controller [2]. The Kinect is used in research to detect hand gestures to use as instructions for HCI. The work proposed by [3], explained how, by using Kinect to capture three-dimensional (3D) images and depth information of foreground objects as input, they could perform hand segmentation and detect the centers of palms using distance transformation on the inverse image. They reported accurate fingertips and center of palm identification, even when the fingers were bent at a large angle. The accuracy for open fingertips detection was almost 100%, whereas center of palm detection was approximately 90% correct. These results demonstrate the effectiveness of the Kinect hand gestures detection. Yao and Fu [4] reported 95.43% accuracy of hand detection with a skin color segmentation procedure. For hand parts classification, they proposed a hand contour model to simplify the gesture matching process when the hand gestures were tracked under unconstrained conditions. The average accuracy of hand parts classification was 74.65%. The team evaluated the feasibility and effectiveness in an application using a tangible user interface for organic chemistry education. They concluded that using a Kinect sensor and a 3D hand contour with labeled information provided a simplified hand model to facilitate building a real-time bare hand controlled interface.

The Kinect sensor was primarily designed for natural interaction in computer game environments [5]. However, since its launch, this MGS has provided great progress in human body tracking, face recognition, and robust hand gesture recognition research [6]. The Kinect sensor has also been assessed for its practical accuracy and precision. Gonzalez-Jorge et al. [7] compared the Kinect and Xtion sensors. Accuracy and precision tests show no dependence on the type of sensor (two Kinect and one Xtion are used for the experiment) or with the incident angle between the standard artifact and the sensor. Distance caused a decrease in accuracy and precision following a second order polynomial. At

* Corresponding author.
E-mail addresses: jgonzalezba@ipn.mx, gonzbarjj@gmail.com (J.-J. González-Barbosa).

http://dx.doi.org/10.1016/j.measurement.2016.07.017
0263-2241/

ranges exceeding 7 m, the sensors could not provide any measure. However, at 1 m range, the accuracy was 5–15 mm and 5–25 mm for 2 m range. The reported precision data for the 1 and 2 m ranges were 1–6 mm and 4–14 mm, respectively. These results confirm the practicality of the Kinect sensor in engineering applications, provided the measurement range is short and the required accuracy is not too strict.

Another consumer-grade MGS is the Leap Motion Controller (LMC), launched in mid-2013 [8,9]. LMC focuses only on hand gesture recognition, and allows users to interact with the computer through those hand gestures [10]. This sensor introduces high-precision hand and finger tracking as a desktop NUI to improve the HCI [11]. According to the manufacturer, LMC is able to recognize gestures and the position of the hands [12], with sub-millimeter accuracy (0.01 mm) [13].

LMC accuracy is due to a combination of vision and proximity based systems. The vision based system consists of two embedded CCD cameras [14] that acquire basic natural hand gestures without touching the device [15]. The proximity based system consists of three infrared LEDs [14], to measure the distance of the hand or another pointer object to LMC. The proximity based system detects reflected IR light, whose intensity increases as the object distance decreases, reducing the power consumption of gesture recognition [15].

To understand LMC functionality, we can refer to the first work that used the preliminary version of the sensor [14]. A precise reference system was needed to evaluate the accuracy and repeatability of the LMC, with measurements in accordance to ISO 9283. They tracked a reference pen tip simultaneously by the robot and the LMC. The results demonstrated an axis-independent deviation for static setups between the desired 3D position and the measured position of less than 0.2 mm. For dynamic situations, independent from the plane, the accuracy was less than 2.5 mm. Repeatability averaged less than 0.17 mm. They concluded it was not possible to achieve the theoretical accuracy of 0.01 mm under real conditions but it did provide high precision (0.7 mm).

Jože Guna et al. [16] systematically analyzed the sensory space and defined the spatial dependency of LMC, its accuracy and reliability. A set of static and dynamic measurements were performed with different numbers of tracking objects and configurations. For static measurements, a plastic arm model simulating a human arm was used, and showed a standard deviation less than 0.5 mm. For dynamic measurements, a special V-shaped tool, consisting of two tracking objects maintaining a constant distance between them, was created to simulate two human fingers. This revealed inconsistent performance of the controller. They concluded that the controller in its current state could not be used as a professional tracking system, primarily due to its rather limited sensory space and inconsistent sampling frequency. Both works agreed that LMC represents a revolutionary input device for gesture HCI. However, [16,14] found several negative characteristics to consider in regard of the LMC: accuracy, axis-independent deviation, inconsistent sampling frequency, and rather limited sensory space.

Cho and Lee [17] and Yulong Xi et al. [18] showed that while the LMC has disadvantages, even with these the LMC can be considered as a NUI in studies requiring low precision, because it simplifies the HCI. Yulong Xi et al. [18] proposed a trap algorithm to correct the palm coordinate instability when the palm simulates touching a surface at a distance of 300 mm. They verified the feasibility of the trap algorithm, implementing the proposed approach and experimenting with a projected coffee menu application program. They concluded the proposed approach overcame the disadvantages present in the LMC. However, while the palm was properly recognized within 300 mm of the LMC, palm coordinates were very unstable during the process when the palm touched the surface.

Cho and Lee [17] developed a serious game for children using the LMC based on the honey bee dance. They confirmed that hand movement is good for brain development of children, and so claimed their proposed system could offer a new development direction of serious games, promoting the LMC as affordable, with convenient structure and serious game capability.

This work assesses 3D verification with a polynomial correction of the LMC for hand gesture recognition. Our methodology is based on ISO 10360-2:2009 [19], and a calibrated coordinated measuring machine (CMM) manufactured by SIP (Société d'Instruments de Précision SA, 19, Rue du Pré-de-la-Fontaine, 1217 Meyrin, Switzerland) was used as the 3D reference position. CMM software alignment was used to align the LMC with respect to the CMM, the ICP algorithm was used to enhance the alignment with the polynomial tendency incorporated as a linear correction. This will assist determining the absolute positions of the vector that represents the pointer device in the LMC field of view. Our results show the advantage of using probabilistic positions once the uncertainty and accuracy of the data acquired from the LMC is known.

2. Materials and methods

2.1. Hand gesture recognition device

Schematics of the main components of the LMC and its field of view are shown in Fig. 1, with the components and physical dimensions of the LMC shown in Fig. 1a. Two CCD cameras and three IR LEDs detect an object (e.g. a finger or pointer) in the field of view. The stereographic camera arrangement complements the IR LEDs to prevent losing track of objects within the field of view and at the same time creates a 3D interaction space.

Fig. 1b and c shows the maximum values for the field of view volume. The maximum distance tolerances per axis are: 609.6 mm, length or X axis; 342.9 mm, height or Y axis; and 300 mm, width or Z axis. The vision angles are 150°, length; 120°, width [13,12,20].

2.2. Experimental setup

Ground-truth was established using a metrologically traceable instrument: SIP-CMM5 (see Fig. 2a) from the three-dimensional laboratory CENAM. The laboratory has a controlled environment at 20 ± 0.2 °C and 58,800 lumen lighting supplied by 28 fluorescent sources with total power 35 W.

The SIP-CMM5 has repeatability of 0.2 μm [21], and maximum permitted error, linear and volumetric [21],

$$G_L[\mu\text{m}] = 0.5 + \frac{L}{1200}, \tag{1}$$

and

$$G_V[\mu\text{m}] = 0.8 + \frac{L}{800}, \tag{2}$$

where $L = 200$ mm; $G_L = 0.6$ μm and $G_V = 1.05$ μm.

Fig. 2b shows an aluminum cylinder 70 mm long and 16 mm diameter, simulating a finger or pointer. The cylinder reference frame is marked in yellow arrows, and the cylinder was covered with matte anti-reflective tape, to improve detection and tracking.

2.3. Measurement methodology

The methodology for dimensional verification was based on ISO 10360-2-2009 [19]. Calculation of the uncertainty or error was based on [22],

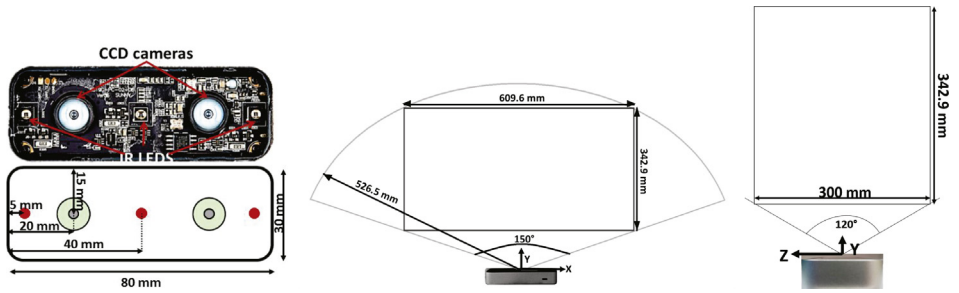

(a) Schematic view. (b) XY field of view. (c) YZ field of view.

Fig. 1. Leap Motion Controller (LMC).

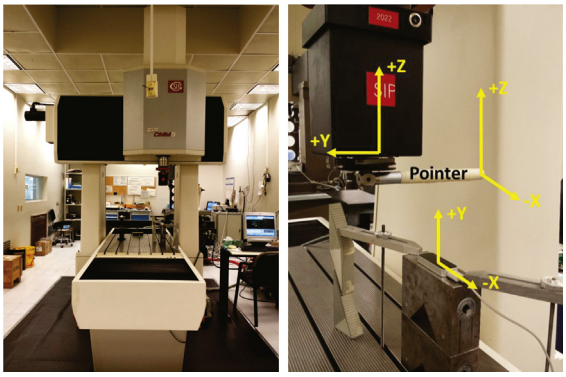

(a) SIP-CMM5. (b) Pointer device.

Fig. 2. Dimensional laboratory and testing artifact.

$$U = k \cdot u_c(y) = k \cdot \sqrt{u_{cal}^2 + u_p^2 + u_w^2} + |b|, \quad (3)$$

where k is the coverture factor, with a conventional value of 2, to achieve a confidence probability of 94.5% in the calculated uncertainty; $u_c(y)$ is the combined standard uncertainty of the estimate y, where y is the estimate of the measurand; u_{cal} is the standard calibration uncertainty of the reference standard to be measured, the SIP-CMM5, explained in Section 2.2; u_p is the standard uncertainty of the sum of errors in the measurement process, obtained from the samples acquired at each point, explained below; u_w is the standard uncertainty of manufacture, these LMC values were calculated with an instrumental drift for each axis.

The systematic error is

$$b = \bar{x} - x_{cal}, \quad (4)$$

and was corrected in each axis after the calibration of the CMM. Thus, in our uncertainty calculation, $b = 0$. If the error were not corrected it would be necessary to include b.

The methodology, shown in Fig. 3, has three steps.

1. Alignment
   Alignment. Using the CMM capabilities, the pointer device was placed at six different points along the LMC field of view: three points along the Z axis, two on the Y axis and one on the X axis (see Fig. 4a), giving a mean distance of 273.480 mm between the points of CMM and LMC points. CMM best fit software was used to align the frameworks due to the spatial distance between them.
   Realignment. To improve the alignment, nine points which define a cube were marked inside the field of view of LMC and the distances between the CMM and the LMC points were calculated (see Fig. 4b). The mean distance between points was 13.734 mm.
   Iterative Closest Point Algorithm. The ICP algorithm was used to further align CMM and LMC points. We also obtained the rigid transform data (rotation matrix and translation vector) of the LMC framework with respect to the CMM reference frame. The mean distance after applying the algorithm was 12.202 mm.

   The rotation and translation vectors obtained from the ICP algorithm were introduced into the CMM software to obtain the linkage of the frameworks.
2. 1D Pre-verification and Correction
   Dimensional pre-verification. Once the frameworks had been aligned, the pre-verification considered only three paths parallel to each axis. Five points were marked on each path and measured three times.
   Polynomial tendency correction. A polynomial tendency correction was fitted to the five points using the average of the three measurements average (Fig. 5). The polynomial for each axis was calculated and passed to a C++ program to obtain corrected positions from the LMC for future measurements of pointer or finger location.
3. Verification based on ISO 10360-2:2009
   One dimensional verification. Five points, measured three times, were acquired parallel to LMC axes for dimensional pre-verification. The error and uncertainty were calculated using Eq. (3).
   Three dimensional verification. Sixty measured points, comprising four different trajectories with three measurements per point, were acquired to calculate the error and uncertainty of the 3D behavior of the LMC field of view. Fig. 7 shows these trajectories and the error between the LMC and CMM reference points.

3. Results and discussion

3.1. Instrumental drift

To obtain the standard uncertainty of the variations of LMC, we implemented an instrumental drift at each axis over 3 and 15 h. The LMC was placed 200 mm under the pointer device which was positioned at point (0, 150, 5) in the LMC field of view (see Fig. 2b). The instrument drift over 3 and 15 h are shown in Table 1.

Frank Weichert et al. [14] obtained an axis-independent deviation in the static test between a desired 3D position and the LMC measured positions of less than 0.2 mm (in particular, 0.17 mm in the X axis), whereas we show a dependency between the Y and Z axes with minimum mean variation along the X axis 0.7 mm and mean deviation of 0.026 mm.

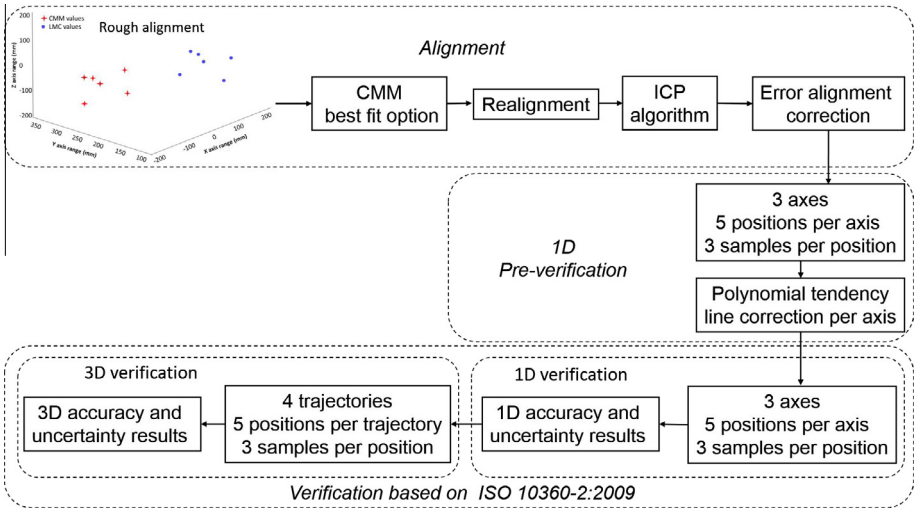

Fig. 3. Measurement methodology.

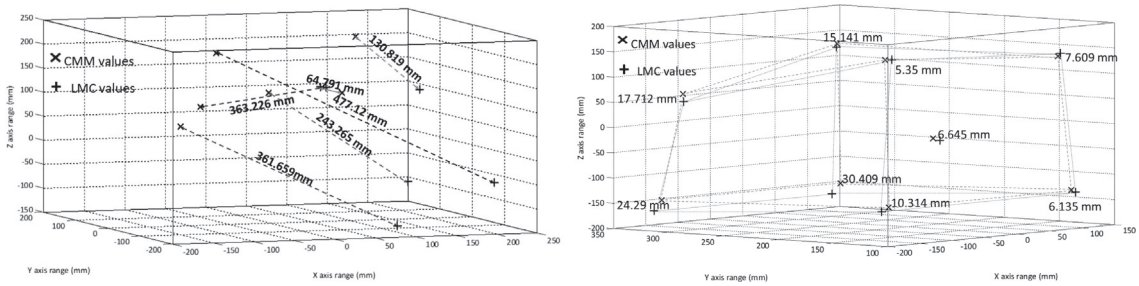

(a) Alignment. (b) Realignment.

Fig. 4. Alignment and realignment distance between LMC and CMM points.

3.2. Alignment

Fig. 4a shows the original distance between the LMC and CMM reference points, derived for frameworks in different positions. The maximum distance was 477.120 mm, minimum 64.791 mm, and the mean distance of the six points was 273.480 mm. After alignment and applying the CMM best fit software option (see Fig. 4b), the maximum distance was reduced by 446.711–30.409 mm. The minimum distance reduced 59.441–5.350 mm, and the mean distance reduced to 13.734 mm. To improve these distances further, we applied the ICP algorithm.

3.2.1. ICP algorithm results

The ICP algorithm was based on [23]. After applying ICP, the mean distance reduced to 12.202 mm, improving by 0.291 mm. The rotation matrix R_{ICP} and translation vector T_{ICP} obtained from the ICP algorithm were, respectively,

$$R_{ICP} = \begin{bmatrix} 0.9999 & -0.0110 & 0.0058 \\ 0.0111 & 0.9998 & -0.0161 \\ -0.0057 & 0.0161 & 0.9999 \end{bmatrix}, \quad (5)$$

and

$$T_{ICP} = \begin{bmatrix} -0.9992 \\ -2.6947 \\ 5.2391 \end{bmatrix}. \quad (6)$$

We transformed the ICP rotation matrix, R_{ICP}, to the rotation vector $R_{Rodrigues}$ using the program of [24], based on Rodrigues algorithm,

$$R_{Rodrigues} = \begin{bmatrix} 0.9233 \\ 0.3295 \\ 0.6327 \end{bmatrix}. \quad (7)$$

The $R_{Rodrigues}$ and T_{ICP} vectors were introduced as rotation and translation parameters, respectively, into the SIP-CMM5 software, and the CMM framework was virtually rotated and translated into the LMC framework. One dimensional pre-verification was performed to ensure the rigid transformation was correct.

3.3. 1D pre-verification and correction

The polynomial tendency correction was the specific treatment selected by the presence of a trend component in the axes (see Fig. 5). Fig. 5a shows the characteristics required to choose a polynomial adjustment: increasing and decreasing slope of structure and variable arrangement.

Fig. 5 shows the error behavior in the various axes before and after the polynomial tendency correction, and Table 2 shows the errors between the reference point and the LMC acquired point.

The 1D pre-verification provides the scale factors in each axis and identifies the errors and uncertainties with the polynomial correction.

3.4. 1D dimensional verification

The *X* axis positions in Fig. 6a have error 0.098 mm, and uncertainty 0.093 mm.

Fig. 6b shows the *Y* axis position with mean error 2.596 mm, And uncertainty 0.156 mm.

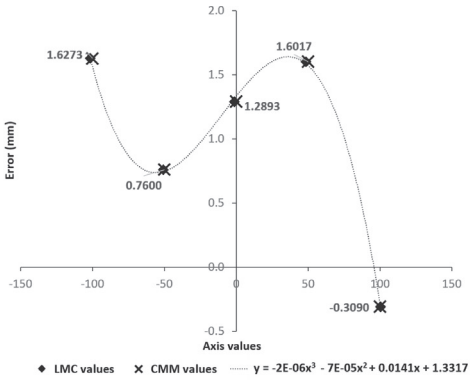

(a) Error without correction, X axis.

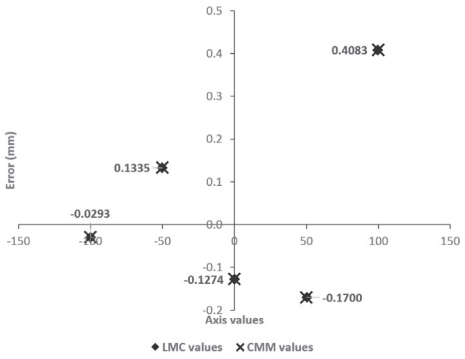

(b) Error after polynomial correction, X axis.

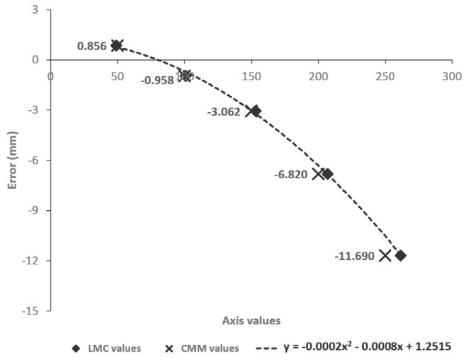

(c) Error without correction, Y axis.

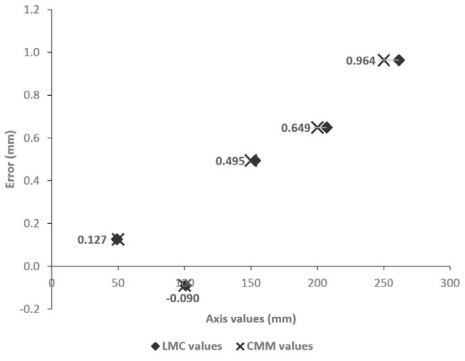

(d) Error after polynomial correction, Y axis.

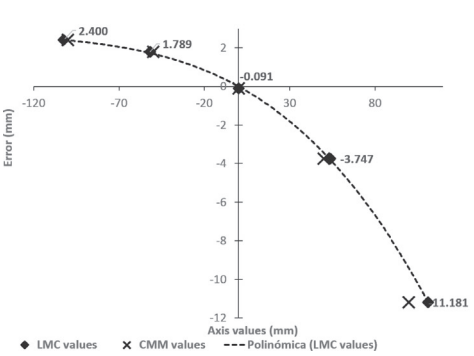

(e) Error without correction, Z axis.

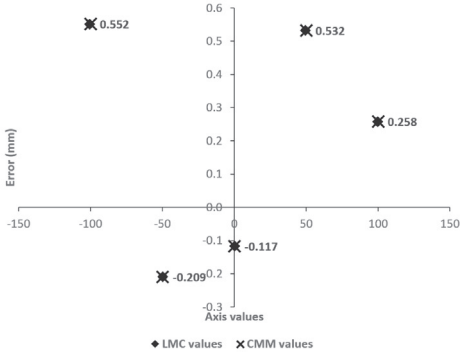

(f) Error after polynomial correction, Z axis.

Fig. 5. Errors before and after the polynomial tendency correction.

Table 1
LMC instrumental drift per axis with respect to the known position (0, 150, 5).

Metric	X axis (mm)	Y axis (mm)	Z axis (mm)
$Variation_{3hours}$	−0.690	148.781	4.106
$Variation_{15hours}$	−0.717	148.508	4.052
$Error_{3hours}$	0.690	1.218	0.893
$Error_{15hours}$	0.717	1.492	0.948
σ_{3hours}	0.023	0.215	0.306
$\sigma_{15hours}$	0.029	0.390	1.073

Table 2
Previous error and error with uncertainties after polynomial correction in each axis.

Axis	Results after correction		
	Previous mean error (mm)	Mean error (mm)	Uncertainty (mm)
X	0.993	0.043	0.133
Y	4.335	10.429	0.386
Z	2.166	0.203	0.177

The Z axis (Fig. 6c) has mean error 0.003 and uncertainty 0.215 mm.

3.5. 3D verification

The trajectories simulate an easy finger movement (Fig. 7). The first trajectory represents an up and down path (Fig. 7a), the fourth is a slice action, from upper left to bottom right (Fig. 7d). The second and third trajectories recreate a check action, from upper left to the bottom and up to the right (Fig. 7b and c, respectively). All the trajectories were performed inside the LMC field of view. Table 3 shows the 3D verification of each trajectory.

These errors are the deviation of LMC tracked data from a desired 3D position measured by the CMM. The mean error of

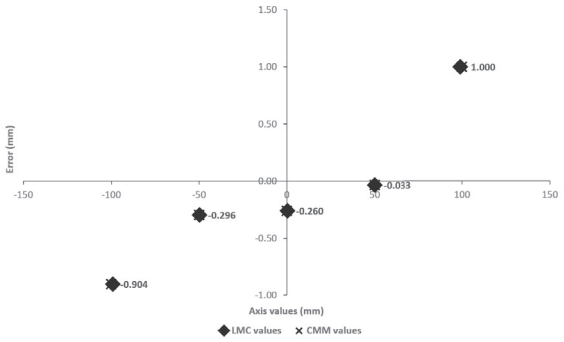

(a) X axis.

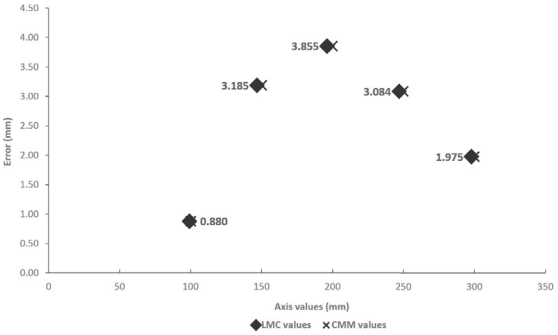

(b) Y axis.

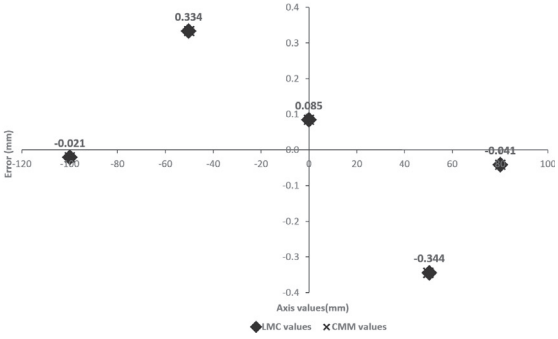

(c) Z axis.

Fig. 6. Errors from parallel paths to the axis.

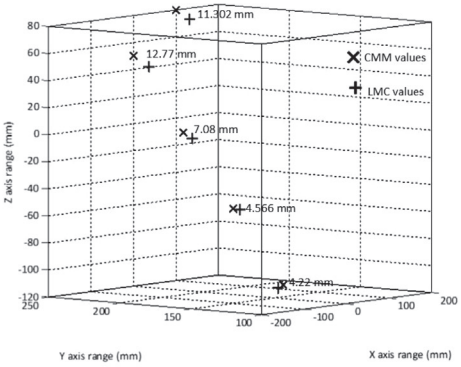

(a) Trajectory 1

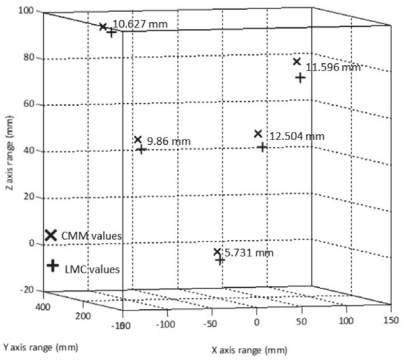

(b) Trajectory 2

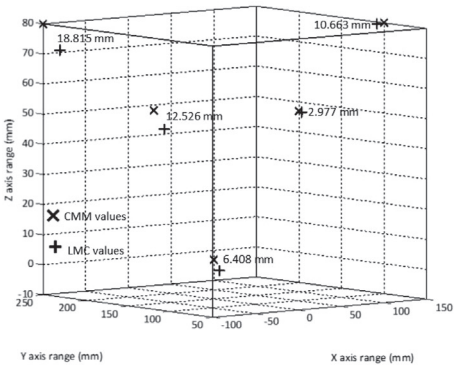

(c) Trajectory 3

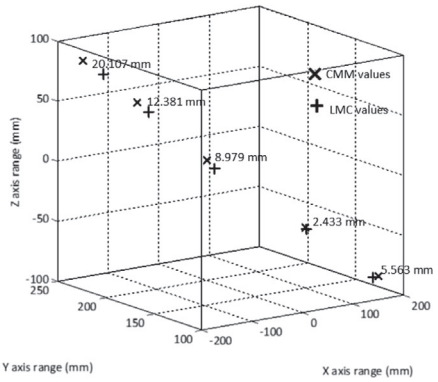

(d) Trajectory 4

Fig. 7. CMM and LMC 3D positions.

Table 3
Errors for the 4 trajectories, 3D verification.

Trajectory	Error			
	Mean (mm)	Maximum (mm)	Minimum (mm)	Uncertainty (mm)
First	7.987	12.770	4.220	0.136
Second	10.064	12.504	5.731	0.198
Third	10.278	18.815	2.977	0.643
Fourth	9.893	20.107	2.433	0.139

the four trajectories was 9.550 mm, significantly larger than the quoted manufacturing accuracy, 0.01 mm [13]. The uncertainties also exceed 0.01 mm, the smallest being 0.136 mm in the first trajectory. Other researchers [14,16] have commented previously regarding the manufacturing accuracy. When [14] moved a sharp pen mounted on the robotic arm over discrete positions on a path, the standard deviation was slightly less than 0.7 mm per axis, implying it was not possible to achieve the nominal manufacturing accuracy of 0.01 mm under real conditions.

4. Conclusions

We propose dimensional verification of the LMC framework, using a CMM scheme as the known reference frame and based on ISO 10360-2:2009. Since the position determined by the sensor has a direct influence on the quality of gesture recognition [14], our verification focused on the error and uncertainty of determining the distance of each axis and four different 3D trajectories compared with a known position.

Significant uncertainty persists in the 1D and 3D verifications, even after the polynomial correction. This uncertainty should be reduced to the minimum required by the application. We proposed the polynomial correction but this could also be achieved using uncertainty models, particle filtering, or probability density models. These models would provide a robust tracking framework suitable for gesture recognition systems [25]. The error compensation techniques mentioned in [26] could then be applied on the corrected data.

Different methodologies and equipment could be employed to measure the error and uncertainty, such as those proposed by [27], using an interferometer suitable for the highest accuracy demands. Use of an interferometer would not limit the maximum size of the working volume. It would also not require any alignment of equipment and yields a very simple data structure, which could be evaluated by appropriate software. The correction of the position uncertainties from LMC were not improved by our proposed scheme. For future work we will develop probabilistic models for gesture recognition, building on the results here. This work demonstrated the error and uncertainties in positioning performance of the LMC in 1D and 3D. LMC requires additional tracking models and position error compensation for applications requiring high accuracy, such as industrial processes or surgical procedure simulations.

Acknowledgements

The authors thank Consejo Nacional de Ciencia y Tecnologa (CONACYT) for the scholarships awarded (227445 and 39479), Instituto Politécnico Nacional (IPN) particularly at Centro de Investigación en Ciencia Aplicada y Tecnología Avanzada Unidad Querétaro (CICATA-Qro) for the financial support given, and Centro Nacional de Metrología (CENAM) for the facilities granted.

References

[1] W. Yi Beifang, Harris Frederick, Yan Yusong, Real-time natural hand gestures, Comput. Sci. Eng. 7 (3) (2005) 92–96 (English).
[2] Jungong Han, Ling Shao, Jamie Shorting, Enhanced computer vision with microsoft kinect sensor: a review, IEEE T. Syst. Man Cy B 43 (5) (2013) 1318–1334, http://dx.doi.org/10.1109/TCYB.2013.2265378.
[3] C. Raheja Jagdish, L. Singal Kunal, Tracking of fingertips and centres of palm using KINECT, in: 2011 Third International Conference on Computational Intelligence, Modelling and Simulation (CIMSiM), 2011, pp. 248–252, http://dx.doi.org/10.1109/CIMSim.2011.51 (English).
[4] Yuan Yao, Yun Fu, Contour model-based hand-gesture recognition using the kinect sensor, IEEE Trans. Circ. Syst. Video Technol. 24 (11) (2014) 1935–1944, http://dx.doi.org/10.1109/TCSVT.2014.2302538 (English).
[5] K. Khoshelham, Accuracy Analysis Of Kinect Depth Data, in: Remote Sensing and Spatial Information Sciences Workshop, August 2011 (English).
[6] J. Zhou Ren, Junsong Yuan, Zhengyou Zhang, Robust part-based hand gesture recognition using kinect sensor, IEEE Trans. Multimedia 15 (5) (2013) 1110–1120, http://dx.doi.org/10.1109/TMM.2013.2246148 (English).
[7] E.J.H. Gonzalez-Jorge, B. Riveiro, P. Arias, Metrological evaluation of Microsoft Kinect and Asus Xtion sensors, Measurement 46 (2013) (English).
[8] Scott Nichols, Michelle Fitzsimmons, From Techradar: Leap Motion Shoves Release of Gesture Control Tech to Late July.
[9] Leap Motion, Section: Blog, Update Shipping this Week and Authorizing Credit Cards.
[10] M. Spiegelmock, Leap Motion Development Essentials (English).
[11] N. Bacim Felipe, A. Bowman Doug, Slice-n-Swipe: a free-hand gesture user interface for 3D point cloud annotation, in: 2014 IEEE Symposium on 3D User Interfaces (3DUI), 2014, pp. 185–186, http://dx.doi.org/10.1109/3DUI.2014.6798882 (English).
[12] Hearst Electronic Products, Fundamentals Behind New Product Leap Motion, and its Natural User Interface Technology, 2013. <http://www.electronicproducts.com/PrintArticle.aspx?ArticleID=60394>.
[13] Leap Motion, Section: Product, 2013. <https://www.leapmotion.com/product>.
[14] B. Frank Weichert, Daniel Bachmann, Denis Fisseler, Analysis of the accuracy and robustness of the leap motion controller, SENSORS 13 (2013) 6380–6393, http://dx.doi.org/10.3390/s130506380 (English).
[15] A.E. Heng-Tze Cheng, An Mei Chen, Contactless gesture recognition system using proximity sensors, in: 2011 IEEE International Conference on Consumer Electronics (ICCE), 2011, pp. 149–150, http://dx.doi.org/10.1109/ICCE.2011.5722510 (English).
[16] M.S. Jože Guna, Grega Jakus, J. Sodnik, An analysis of the precision and reliability of the leap motion sensor and its suitability for static and dynamic tracking, SENSORS 14 (2014) 3702–3720, http://dx.doi.org/10.3390/s140203702 (English).
[17] Ok-Hue Cho, Sung-Tae Lee, A study about honey bee dance serious game for kids using hand gesture, IJMUE J. 9 (8) (2014) 397–404, http://dx.doi.org/10.1023/A:1008078328650 (English).
[18] Y.K. Yulong Xi, Seoungjae Cho, Kyhyun Um, Surface touch interaction method using inverted leap motion device, in: Future Information Technology, Lecture Notes in Electrical Engineering, vol. 309, Springer, Berlin, Heidelberg, 2014, pp. 469–474 (English).
[19] ISO 10360-2:2009, Geometrical Product Specification (gps), Acceptance and Reverification Tests for Coordinate Measuring Machines (cmm). Part 2: Cmms Used for Measuring Linear Dimensions, 2009.
[20] I. Westminster Technologies, Hearst Electronic Products, Leap Motion: Interaction Area, 2014. <http://www.westminstertech.com/leap-motion/>.
[21] BACH TOOL Precision, Sip (Swiss) cmm Machine, 2012. <http://www.bachtoolprecision.com/metrology.php>.
[22] JCGM 100:2008, Evaluation of Measurement Data: Guide to the Expression of Uncertainty in Measurement, 2009.
[23] Wilm Jakob, Kjer Hans, Evaluation of Surface Registration Algorithms for Pet Motion Correction, Bachelor Thesis, Technical University of Denmark, informatics and Mathematical Modelling, 2010.
[24] Serge Belongie, Rodrigues Rotation Formula, From MathWorld–A Wolfram Web Resource, created by Eric W. Weisstein, 2013. <http://mathworld.wolfram.com/RodriguesRotationFormula.html>.
[25] Isard Michael, Blake Andrew, CONDENSATION: conditional density propagation for visual tracking, Int. J. Comput. Vis. 29 (1) (1998) 5–28, http://dx.doi.org/10.1023/A:1008078328650 (English).
[26] Robert J. Hocken, Paulo H. Pereira, Coordinate Measuring Machines and Systems, 2012 (English).
[27] J.H. Schwenke, M. Franke, H. Kunzmann, Error mapping of CMMs and machine tools by a single tracking interferometer, Cirp. Ann. Manuf. Technol. 54 (1) (2005) 475–478, http://dx.doi.org/10.1016/S0007-8506(07)60148-6 (English).